Engineering Science and Technology, an International Journal 19 (2016) 40–44

HOSTED BY

Contents lists available at ScienceDirect

Engineering Science and Technology, an International Journal

journal homepage: http://www.elsevier.com/locate/jestch

Full Length Article

Effect of particle size on dc conductivity, activation energy and diffusion coefficient of lithium iron phosphate in Li-ion cells

T.V.S.L. Satyavani [a,*], B. Ramya Kiran [b], V. Rajesh Kumar [a], A. Srinivas Kumar [a], S.V. Naidu [b]

[a] N.S.T.L., Vigyan nagar, Visakhapaatnam, India
[b] Department of Chemical Engineering, Andhra University, Visakhapatnam, India

ARTICLE INFO

Article history:
Received 24 March 2015
Received in revised form
27 May 2015
Accepted 29 May 2015
Available online 8 August 2015

Keywords:
Activation energy
dc conductivity
ac impedance and diffusion coefficient

ABSTRACT

Cathode materials in nano size improve the performance of batteries due to the increased reaction rate and short diffusion lengths. Lithium Iron Phosphate ($LiFePO_4$) is a promising cathode material for Li-ion batteries. However, it has its own limitations such as low conductivity and low diffusion coefficient which lead to high impedance due to which its application is restricted in batteries. In the present work, increase of conductivity with decreasing particle size of $LiFePO_4$/C is studied. Also, the dependence of conductivity and activation energy for hopping of small polaron in $LiFePO_4$/C on variation of particle size is investigated. The micro sized cathode material is ball milled for different durations to reduce the particle size to nano level. The material is characterized for its structure and particle size. The resistivities/dc conductivities of the pellets are measured using four probe technique at different temperatures, up to 150 °C. The activation energies corresponding to different particle sizes are calculated using Arrhenius equation. CR2032 cells are fabricated and electrochemical characteristics, namely, ac impedance and diffusion coefficients, are studied.

1. Introduction

Nano materials are expected to play a key role in the performance improvement of rechargeable Li-ion battery technology. Nano materials increase the surface area, leading to higher electrode–electrolyte contact and thus enhance the reaction rate. The solid state diffusion of Li-ions is generally considered to be the rate-determining step of Li-ion batteries. Therefore, the nano structured materials are extensively explored in an effort to enhance the kinetic properties by decreasing the diffusion length to a nanometer scale. Due to the short diffusion length, the nano structured materials show high rate performances [1]. The lithiated olivine phosphates are promising new generation cathode materials for Li-ion rechargeable batteries owing to their numerous advantages such as high energy density, low cost and environmental friendliness. Ever since it is synthesized, the lithium iron phosphate ($LiFePO_4$ or LFP) became a very promising choice of cathode materials [2]. It exhibits reversible electrochemical lithium insertion/extraction reactions at ~3.4 V (vs. Li/Li^+) with a theoretical capacity of 170 mAh g^{-1} [3]. During lithium-ion extraction and insertion, the active material undergoes a two-phase transition between $LiFePO_4$ and $FePO_4$, with a flat voltage profile. $LiFePO_4$ is safer as compared to other metal-oxide cathode materials. Additionally, $LiFePO_4$ cathode material lies in its tolerance to overcharge/discharge and less prone to thermal runaway [4]. Also, $LiFePO_4$ has good cycle and thermal stabilities. In spite of its superior performance, $LiFePO_4$ material has to overcome some barriers for practical applications. Among various issues, the most important concern is its low intrinsic electronic conductivity and slow lithium-ion diffusion across the $LiFePO_4/FePO_4$ phase boundary during charge/discharge processes which limit the rate performance of this material. The slow diffusion rate of Li-ion is attributed to a variety of material properties such as large miscibility gap, dimensionality and nature of defect sites [5–9]. Over the past few years, numerous efforts have been made to circumvent the drawbacks mentioned above, including reducing the particle size and homogeneous particle size distribution and supervalent doping [10,11]. An increase by eight orders of magnitude in the electronic conductivity of the olivine-type material is reported by adopting various techniques to increase the conductivity [12–14]. It is generally accepted that the olivine phosphates are wide gap materials in which the charge transport is ascribed by the archetype small polaron hopping rather than band-like transport [15]. The mobile charge carriers can be either electrons or holes in $LiFePO_4$ systems depending on the lithium addition or withdrawal where the mobile charge carriers occupy Fe^{2+}/Fe^{3+} redox couple. The theoretical in-

* Corresponding author. Tel.: +91 8912586129, fax: +91 8912586494.
E-mail address: tvslsatyavani@gmail.com (T.V.S.L. Satyavani).
Peer review under responsibility of Karabuk University.

http://dx.doi.org/10.1016/j.jestch.2015.05.011

vestigations on the polarons in n-dimensional crystals suggest that the polaron effect enhances as the dimensionality of the system reduces. The activation barrier associated with the hopping is found to be a thermally activated process [16]. The enhancement in electronic conductivity of $LiFePO_4$ is due to the lattice strain associated with the reduction of particle size. This becomes prominent at the typical nano scale regime. At nano scale, i.e., particle size of less than 200 nm, there is an enhancement in the polaronic conductivity of about an order of magnitude. The temperature dependence of dc conductivity and nonlinearities in the transport properties of $LiFePO_4$ with particle size are due to the interplay between the confinement and lattice strain. The dependence is also due to the effects of strain on the electron–phonon interactions. Finally, the reduction of particle size leads to a shorter hopping distance. The observed conductivity of $LiFePO_4$ at room temperature is of the order of 10^{-10}–10^{-5} S cm^{-1} [16] with an activation energy (E_a) of about 0.65 eV. The limiting factor for the performance of $LiFePO_4$ based batteries is related to the material's low electrical conductivity, both ionic and electronic. The ionic component of electrical conductivity is related to the mobility of Li^+ ions. It is preferential along [010] direction which is characterized by the E_a of 0.55–0.65 eV when compared to [001] direction with $E_a = 2.89$ eV and [101] direction with $E_a = 3.36$ eV [9,17]. It is observed that there exists a relationship between the electronic and the ionic conductivity in $LiFePO_4$ [9,16,18,19]. Faster transport of the small polaron generally leads to fast diffusion of lithium cations, which hints at their mutual connection. Therefore, high electrical resistivity may be considered responsible for the low values of lithium diffusion coefficient, D. Values of D reported in the literature fall over a wide range from 10^{-16} to 10^{-11} cm^2s^{-1}, and their poor reproducibility indicates the strong influence of the method of preparation of material [9].

Effect of particle size reduction on conductivity, activation energy and diffusion coefficient of $LiFePO_4$/C is studied in this paper using commercial $LiFePO_4$ powder of 5 μm particle sizes. The micron size particles of cathode material were reduced to nano level by ball milling for different durations in a liquid medium. This reduction in the particle size was confirmed by X-ray powder diffraction, particle size analyzer and scanning electron microscopy. The samples with different particle sizes were pelletized, and their dc resistivities were measured from ambient to 150 °C by four-probe setup, and the activation energies were calculated using Arrhenius equation. CR2032 cells are fabricated from un-ball milled $LiFePO_4$/C of 5 μm particle size and the material ball milled for 15 h, which was found to have maximum conductivity. Lithium foil was used as anode. These cells were characterized for ac impedances and diffusion coefficients by electrochemical impedance spectroscopy, and the effect of particle size on these parameters is discussed.

2. Experimental

Commercial $LiFePO_4$/C powder with 10% carbon content (LFP-0, 99.99% purity, MTI, USA) was wet ball milled (Planetary ball mill model Retsch PM 100) with toluene as the milling medium. Ball milling was carried out at a speed of 400 rpm with a ball-to-powder ratio of 10:1 for different durations of 5 (LFP-5), 10 (LFP-10), 15 (LFP-15) and 20 hours (LFP-20) to obtain particles of nano size. The obtained samples were further structurally characterized by X-ray powder diffraction, particle size analyzer and scanning electron microscopy (SEM) using PANalytical x'pert pro X-ray Diffractometer, HORIBA scientific nanopartica SZ-100, nano particle analyzer, and Zeiss Auriga FIB system with Bruker XFlash detector 5030 for SEM respectively.

The four probe method was used to measure the resistivity of LFP powders. The samples with different particle sizes were pelletized and sintered at 700 °C for 8 hours. Pellets of 10 mm diameter and 1.5 mm thickness were used to measure resistivities. The four probe setup has four individually spring loaded probes which are collinear and equally spaced. This technique involves bringing the four equally spaced probes into contact with the material of unknown resistance. The probe array is usually placed in the center of the material. The outer probes are used for passing constant current though the sample. The electric current carried though the two outer probes sets up an electric field in the sample. The two inner probes measure potential difference using a high impedance voltmeter.

The whole arrangement is mounted on a suitable stand and the leads are provided for the voltage measurement. The experimental setup consists of a probe arrangement, sample, oven up to 200 °C, constant current generator, oven power supply and digital panel meter to measure voltage and current. In the present work, constant current sources model nos. CLS-01 and LCS-02 and digital voltmeter DMV-001 connected to a constant temperature chamber/oven (SES Instruments, India) were used for the measurement of resistivity.

Each sintered pellet was kept under the four probes carefully so that all probes rest on the pellet to make proper contact. At room temperature, the resistivity was measured for each pellet. The temperature was increased up to 150 °C with an increment of 10 °C and from the measurements; the resistivity ρ and conductivity σ are calculated corresponding to each temperature. The activation energies were calculated using the following Arrhenius equation [20] and compared with respect to their particle size.

$$\sigma = A exp(-E_a/kT) \quad (1)$$

where, $\boldsymbol{\sigma}$ = Conductivity (S/cm),

$\boldsymbol{E_a}$ = Activation energy (eV)
$\boldsymbol{T}$ = Temperature (°K)
$\boldsymbol{k}$ = Boltzmann's constant

80 wt% of ball milled $LiFePO_4$/C, 5 wt% of acetylene black and 15 wt% poly vinylidene fluoride (PVdF) in *N*-methyl-2-pyrrolidene (NMP) solution was considered to prepare the cathodes. CR 2032 hardware with lithium metal foil as anode (99.9% purity, MTI, USA) was used to fabricate coin cells in half cell configuration [21]. The cells were charged up to 4.2 V and discharged to 2.7 V at room temperature initially for five cycles. The electrochemical characteristics, namely, ac impedance and diffusion coefficient are studied.

3. Results and discussion

The particle sizes obtained from the distribution graph of LFP-5, LFP-10, LFP-15 and LFP-20 are 350 ± 7 nm, 183 ± 3.6 nm, 112 ± 2.2 nm and 107 ± 2.1 nm respectively. A typical particle size distribution of LFP-15 is shown in Fig. 1. Particle size of the commercial $LiFePO_4$ powder [GELON LIB GROUP, CHINA, Batch no: 120105] is of 3–5 μm size.

As can be observed from the microstructure and the surface morphology (from SEM), the particles are broken down to smaller size with increasing time of ball milling. The ball milling yields considerably smaller particles of irregular shape with inhomogeneous particle size distribution. Particle size obtained from the micrograph of LFP-15 is approximately 100 nm which is in close agreement with that obtained from the particle size analysis. SEM micrographs of LFP-0 and LFP-15 are shown in Fig. 2.

The variation of the conductivity with temperature is plotted in Fig. 3, as a typical case. Natural logarithm of conductivity, ln (σ) vs. reciprocal of the temperature, 1/T plotted in Fig. 3 shows an increase in the dc conductivity with increasing temperature. The product of slope of plot and Boltzmann constant gives activation energy [20].

Table 1 shows the variation of resistivity and the conductivity values obtained using four probe technique with ball milling time. It can be seen from Table 1 that grinding of material from 0 to 20

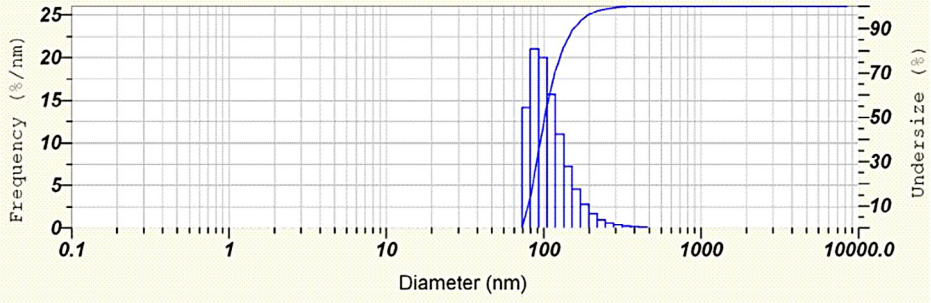

Fig. 1. Particle size distribution of LFP-15.

hours progressively reduces the particle size from 5 μm to 107 nm and increased the conductivity from 1.353×10^{-3} to 24.011×10^{-3} S/cm. The observed error in the particle size measurement was found to be less than 2%. It also shows the variation of activation energy from 0.56 eV to 0.26 eV with particle size and milling time. Only marginal improvements in the above parameters between grinding intervals of 15 hours and 20 hours are observed from Table 1. Thus, 15 hours of grinding of the powders is considered to be optimum.

Table 1 shows the increase of conductivity and decrease of the activation energy with the particle size reduction. The activation barrier associated with the hopping is found to be a thermally activated process [16], and the energy to overcome this barrier decreases with increase in temperature.

Since LFP-15 sample has shown better conductivity and lower activation energy, LFP-15 along with LFP-0 are characterized by X-ray diffraction using PANalytical x'pert pro X-ray diffractometer. The XRD patterns of LFP-0 and LFP-15 are shown in Figs. 4 and 5. The crystallite size is obtained by calculating the broadening of the most intense peak of the respective XRD patterns shown in the insets of Figs. 4 and 5. As observed from the figures, the peak of LFP-15 (Full Width at Half Maximum, FWHM = 0.305°) is broader than the peak of LFP-0 (FWHM = 0.0932°) which clearly shows that the crystallite size of LFP-15 is smaller than the LFP-0.

CR 2032 cells are fabricated in half cell configuration [21] to study ac impedance and diffusion coefficients using the electrochemical impedance spectroscopy (EIS) technique with Ivium Technologies Ivium-n-Stat, a multi-channel Potentiostat/Galvanostat with standard integrated impedance analyzer in each channel. To understand

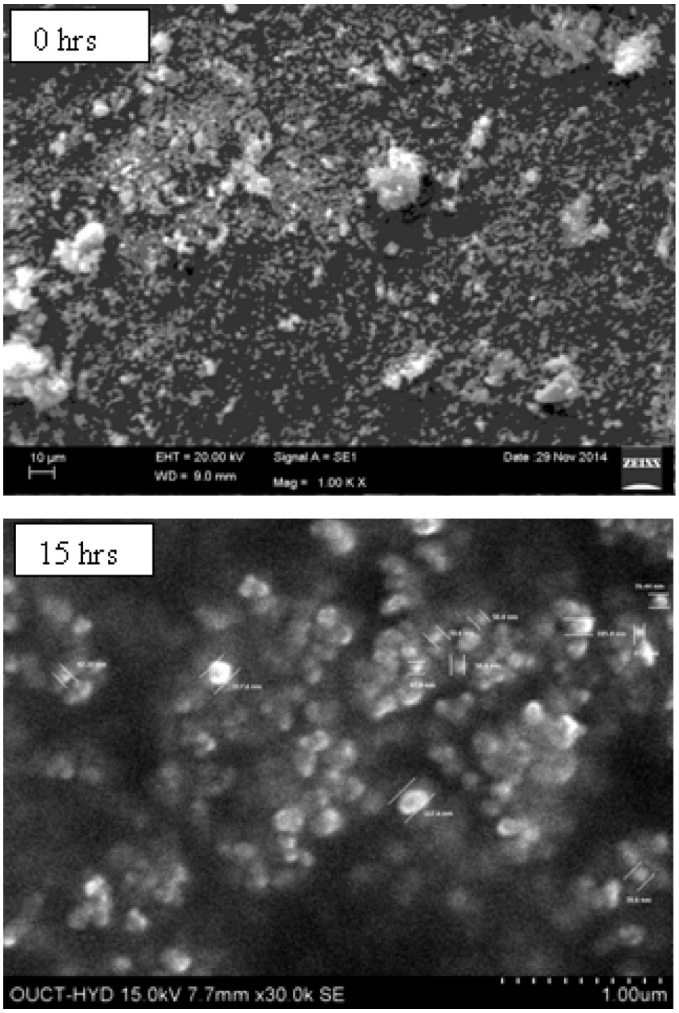

Fig. 2. SEM of LFP- 0 & LFP-15.

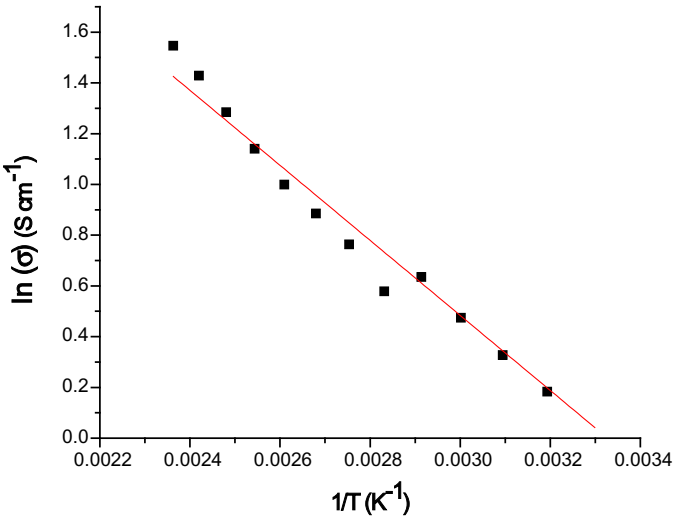

Fig. 3. Plot between ln (σ) and 1/T (K^{-1}).

Table 1
Variation of conductivity and activation energy with particle size.

Time (h)	Particle size (nm)	Conductivity (Scm^{-1})	Activation energy (eV) (eV)
0	5000	1.353×10^{-3}	0.563
5	350 ± 7.0	3.946×10^{-3}	0.559
10	183 ± 3.6	4.244×10^{-3}	0.446
15	112 ± 2.2	23.880×10^{-3}	0.288
20	107 ± 2.1	24.011×10^{-3}	0.256

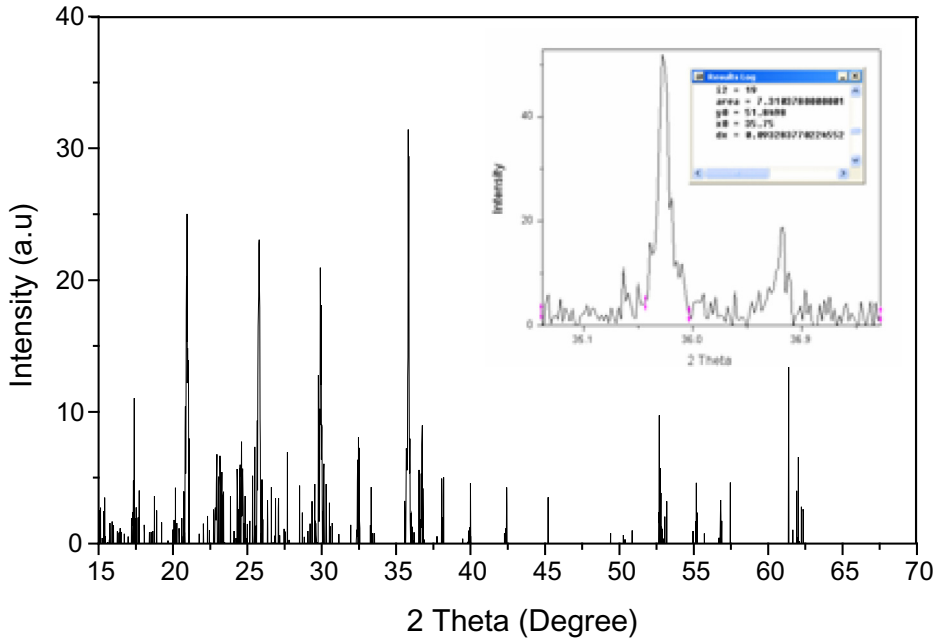

Fig. 4. XRD pattern of LFP-0.

the effect of reduction of particle size in detail, the ac impedance measurement is carried out using the cells containing LFP-0 and LFP-15. The impedance measurement is done after performing galvanostatic cycles five times to confirm the stabilization of SEI film formation and the percolation of electrolyte through electrode particles. Fig. 6 shows Nyquist EIS plots obtained for LFP-0 and LFP-15. An intercept at the Z_{real} axis in the high frequency corresponding to the ohmic resistance R_Ω represents the total resistance of the electrolyte, separator and electrical contacts. The depressed semicircle in the high frequency range is related to the Li-ion migration resistance R_f through the SEI film formed on the electrode. The second semicircle in the middle frequency range indicates the charge transfer resistance R_{ct}. The inclined line in the lower frequency represents the Warburg impedance W, which is associated with the Li-ion diffusion in the $LiFePO_4$ particles.

A simplified equivalent circuit model is constructed to analyze the impedance spectra as shown in the inset of Fig. 6 [22]. Table 2 shows the parameters of the equivalent circuit for LFP-0 and LFP-15. It is observed that the values of R_Ω, R_f and R_{ct} of LFP-15 are reduced considerably after the particle size reduction when compared to LFP-0, suggesting that the overall resistance is decreased and Li-ion diffusion is improved.

Li-ion diffusion coefficients (D_{Li+}) are determined for LFP-0 and LFP-15 using the Warburg coefficients (W) [23] obtained from EIS plots of Fig. 6 and shown in Table 2. There is an improvement of an order of magnitude in the diffusion coefficient from 0.54×10^{-12}

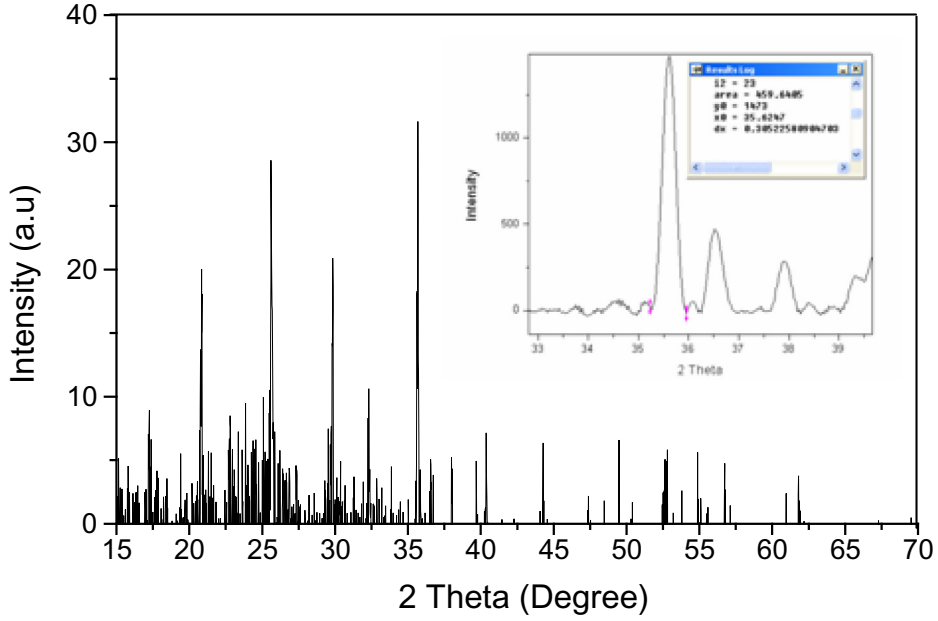

Fig. 5. XRD pattern of LFP-15.

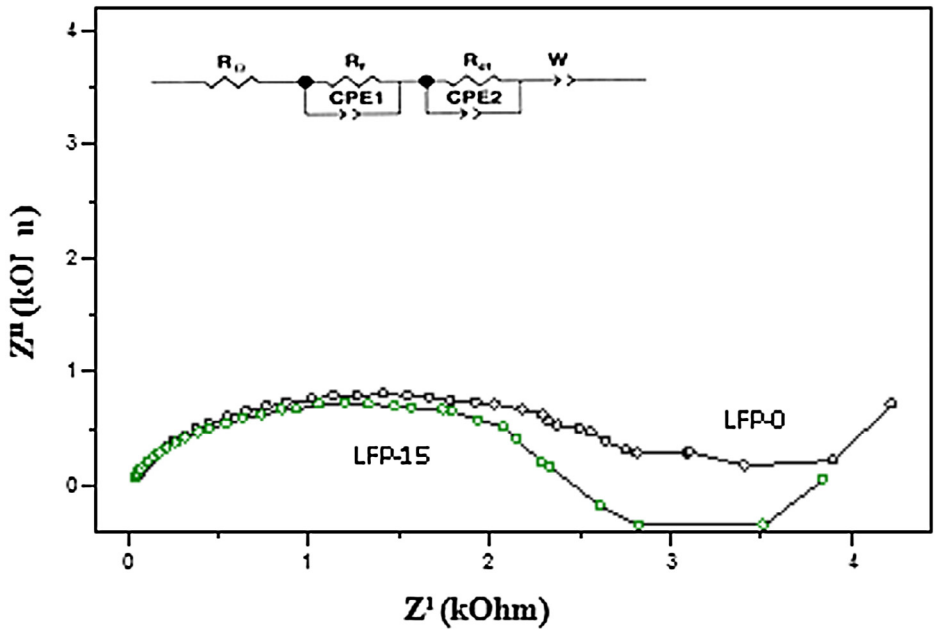

Fig. 6. Nyquist EIS plots of LFP-0 h and LFP-15 h.

to 7.92×10^{-12} cm^2 s^{-1} by particle size reduction. The improved diffusion coefficient is attributed to the shortened diffusion path distance due to particle size reduction and improved electrical conductivity.

4. Conclusions

The effect of particle size reduction on conductivity, activation energy and diffusion coefficient of $LiFePO_4$/C is studied in the present work. Cathode material in micron size is ball milled for different durations to reduce the particle size to nano level. The material is characterized for its structure and particle size. The dc conductivities of pellets are measured at different temperatures up to 150 °C using the four probe setup. Activation energies corresponding to different particle sizes are calculated using Arrhenius equation. The electrochemical characteristics, namely, ac impedance and diffusion coefficient, are studied by fabricating CR2032 cells. It is found that the conductivity and diffusion coefficient increased by an order of magnitude, and activation energy is reduced by half by reducing the particle size from micro level to nano level.

Table 2
Parameters of ac impedance.

Cell no	R(ohmic) (Ω)	R_f (Ω)	R_{ct} (Ω)	W (1/ohm $Hz^{1/2}$)	Diffusion coefficient (cm^2 s^{-1})
LFP-0	187.8	1699	1152.0	294.20	0.54×10^{-12}
LFP-15	128.0	1381	814.3	77.02	7.92 x10^{-12}

References

[1] Y. Wang, H. Li, P. He, E. Hosono, H. Zho, Nanoscale 2 (2010) 1294–1305.
[2] K. Padhi, K.S. Nanjundaswamy, J.B. Goodenough, J. Electrochem. Soc. 144 (1997) 1188–1194.
[3] K. Tang, J. Sun, X. Yu, H. Li, X. Huang, Electrochim. Acta 54 (2009) 6565–6569.
[4] J. Jiang, J.R. Dahn, Electrochem. Commun. 6 (2004) 39–43.
[5] A. Yamada, H. Koizumi, S.I. Nishimura, N. Sonoyama, R. Kanno, M. Yonemura, et al., Nat. Mater. 5 (2006) 357–360.
[6] D. Morgan, A. Van der Ven, G. Ceder, Electrochem. Solid-State Lett. 7 (2004) A30–A32.
[7] M.S. Islam, D.J. Driscoll, C.A.J. Fisher, P.R. Slater, Chem. Mater. 17 (2005) 5085–5092.
[8] S. Nishimura, G. Kobayashi, K. Ohoyama, R. Kanno, M. Yashima, A. Yamada, Nat. Mater. 7 (2008) 707–711.
[9] R. Malik, D. Burch, M. Bazant, G. Ceder, Nano Lett. 10 (2010) 4123–4127.
[10] M. Konarova, I. Taniguchi, J. Power Sources 194 (2009) 1029–1035.
[11] P.S. Herle, B. Ellis, N. Coombs, L.F. Nazar, Nat. Mater. 3 (2004) 147–152.
[12] S.Y. Chung, J.T. Bloking, Y.M. Chiang, Nat. Mater. 1 (2002) 123–128.
[13] S.Y. Chung, Y.-M. Chiang, Electrochem. Solid-State Lett. 6 (12) (2003) A278–A281.
[14] T. Nakamura, Y. Miwa, M. Tabuchi, Y. Yamada, J. Electrochem. Soc. 153 (6) (2006) A1108, 16–17.
[15] S.P. Ong, V.L. Chevrier, G. Ceder, Phys. Rev. B83 (2011) 075112.
[16] R. Shahid, S. Murugavel, Phys. Chem. Chem. Phys. 15 (2013) 18809–18814.
[17] J. Molenda, A. Kulka, A. Milewska, W. Zając, K. Swierczek, Materials 6 (2013) 1656–1687.
[18] B. Ellis, L.K. Pery, D.H. Ryan, L.F. Nazar, J. Am. Chem. Soc. 128 (2006) 11416–11422.
[19] J. Lee, S.J. Pennycook, S.T. Pantelides, Appl. Phys. Lett. 101 (2012) 033901, 1–4.
[20] L.K. Sudha, S. Roy, K.U. Rao, IJMMM 2 (1) (2014) 96–100.
[21] T.V.S.L. Satyavani, A. Srinivas Kumar, P.S.V. Subbarao, Physics of Semiconductor Devices, Environmental Science and Engineering, Springer International Publishing, Switzerland, 2014, pp. 721–723.
[22] H.C. Shin, W.I. Cho, H. Jang, J. Power Sources 159 (2006) 1383–1388.
[23] D.J. Kim, R. Ponraj, A.G. Kannan, H.-W. Lee, R. Fathi, R. Ruffo, et al., J. Power Sources 244 (2013) 758–763.